

Mid-IR Properties of Seyferts: *Spitzer* IRS Spectroscopy of the *IRAS* 12 μm Seyfert Sample

Vassilis Charmandaris^{1,2}, Yanling Wu³, Jiasheng Huang⁴,
Luigi Spinoglio^{5,6}, and Silvia Tommasin^{5,6}

¹University of Crete, Department of Physics, GR-71003, Heraklion, Greece
Email: vassilis@physics.uoc.gr

²IESL/Foundation for Research and Technology - Hellas, GR-71110, Heraklion, Greece, and
Chercheur Associé, Observatoire de Paris, F-75014, Paris, France

³Infrared Processing and Analysis Center, Caltech, Pasadena, CA 91125, USA

⁴Harvard-Smithsonian Center for Astrophysics, Cambridge, MA 02138, USA

⁵Istituto di Fisica dello Spazio Interplanetario, INAF, I-00133 Rome, Italy

⁶Dipartimento di Fisica, Università di Roma, La Sapienza, Rome, Italy

Abstract. We performed an analysis of the mid-infrared properties of the 12 μm Seyfert sample, a complete unbiased 12 μm flux limited sample of local Seyfert galaxies selected from the *IRAS* Faint Source Catalog based on low-resolution spectra obtained with the Infrared Spectrograph (IRS) on-board *Spitzer Space Telescope*. A detailed presentation of this analysis is discussed by Wu *et al.* (2009). We find that, on average, the 15–30 μm slope of the continuum is $\langle\alpha_{15-30}\rangle = -0.85 \pm 0.61$ for Seyfert 1s and -1.53 ± 0.84 for Seyfert 2s, and there is substantial scatter in each type. Moreover, nearly 32% of Seyfert 1s, and 9% of Seyfert 2s, display a peak in the mid-infrared spectrum at 20 μm , which is attributed to an additional hot dust component. The polycyclic aromatic hydrocarbon (PAH) equivalent width decreases with increasing dust temperature, as indicated by the global infrared color of the host galaxies. However, no statistical difference in PAH equivalent width is detected between the two Seyfert types of the same bolometric luminosity. Finally, we propose a new method to estimate the AGN contribution to the integrated 12 μm galaxy emission, by subtracting the “star formation” component in the Seyfert galaxies, making use of the tight correlation between PAH 11.2 μm luminosity and 12 μm luminosity for star forming galaxies.

Keywords. galaxies: active, galaxies: Seyfert, galaxies: nuclei, infrared: galaxies

1. Introduction

Active galaxies emit radiation from their nucleus due to accretion onto a supermassive black hole (SMBH) located at the center. The fraction of the energy emitted from these AGN, compared with the total bolometric emission of the host, can range from a few percent in moderate luminosity systems ($L_{\text{bol}} < 10^{11} L_{\odot}$), to more than 90% in quasars ($L_{\text{bol}} > 10^{12} L_{\odot}$; see Ho 2008 and references therein). As a subclass, Seyfert galaxies are the nearest and apparently brightest AGNs, with 2–10 keV X-ray luminosities less than $\sim 10^{44} \text{ erg s}^{-1}$ and their observed spectral line emission originates principally from highly ionized gas. Seyferts have been studied at many wavelengths and classified as Seyfert 1s (Sy 1s) and Seyfert 2s (Sy 2s), with the type 1s displaying features of both broad (FWHM $> 2000 \text{ km s}^{-1}$) and narrow emission lines, while the type 2s show only narrow-line emission.

The difference between the two Seyfert types has been an intense field of study for many years. Are they due to intrinsic differences in their physical properties, or are they simply

a result of dust obscuration that hides the broad-line region in Sy 2s? A so-called unified model has been proposed (see Antonucci 1993; Urry & Padovani 1995), suggesting that Sy 1s and Sy 2s are essentially the same objects viewed at different angles. A dust torus surrounding the central engine blocks the optical light when viewed edge on (Sy 2s) and allows the nucleus to be seen when viewed face on (Sy 1s). Optical spectra in polarized light (Antonucci & Miller 1985) have indeed demonstrated for several Sy 2s the presence of broad lines, confirming for these objects the validity of the unified model. However, the exact nature of this orientation-dependent obscuration is not clear yet. Recently, more elaborate models, notably those of Elitzur (2008), Nenkova *et al.* (2008), and Thompson *et al.* (2009) suggest that the same observational constraints can also be explained with discrete dense molecular clouds, without the need of a torus geometry.

Mid-IR spectroscopy is a powerful tool with which to examine the nature of the emission from AGNs, as well as the nuclear star-formation activity. Since IR observations are much less affected by dust extinction than those at shorter wavelengths, they have been instrumental in the study of obscured emission from optically thick regions in AGNs. This is crucial to understand the physical process of galaxy evolution. With the advent of the *Infrared Space Observatory (ISO)*, local Seyferts have been studied by several groups (see Verma *et al.* 2005, for a review). The launch of the *Spitzer Space Telescope* (Werner *et al.* 2004) has enabled the study of large samples of AGN with substantially better sensitivity and spatial resolution in an effort to quantify their mid-IR properties (Buchanan *et al.* 2006; Sturm *et al.* 2006; Deo *et al.* 2007; Gorjian *et al.* 2007; Hao *et al.* 2007; Tommasin *et al.* 2008).

We have used archival *Spitzer* IRS (Houck *et al.* 2004) observations and have embarked on a detailed study of the Seyferts in the extended $12\ \mu\text{m}$ galaxy sample. This sample of 116 Seyferts appears to be optimal for studying in an unbiased manner the effects of an AGN on physical properties of a galaxy, since all galaxies emit a nearly constant fraction ($\sim 7\%$) of their bolometric luminosity at $12\ \mu\text{m}$ (Spinoglio & Malkan 1989). A total of 103 Seyferts have been observed by various *Spitzer* programs using the low-resolution ($R \sim 64\text{--}128$) modules of IRS. Among these objects, 47 are optically classified as Sy 1s and 56 as Sy 2s (Rush *et al.* 1993). The details of this work are summarized here and by Wu *et al.* (2009). High-resolution ($R \sim 600$) IRS spectroscopy for 110 objects are also available, and their analysis is presented by Tommasin *et al.* (2008, 2009).

2. Results

2.1. Global Mid-IR Spectra of Seyfert Galaxies

It has been well established that the mid-IR spectra of Seyfert galaxies display a variety of features (see Clavel *et al.* 2000; Verma *et al.* 2005; Weedman *et al.* 2005; Buchanan *et al.* 2006; Hao *et al.* 2007, and references therein). This is understood, since, despite the optical classification of their nuclear activity, emission from the circumnuclear region, as well as from the host galaxy, also influences the integrated mid-IR spectrum of the source.

The IRS spectra of 47 Sy 1s and 54 Sy 2s with full $5.5\text{--}35\ \mu\text{m}$ spectral coverage, normalized at the wavelength of $22\ \mu\text{m}$, are averaged and plotted in Figure 1. For comparison, we over-plot the average starburst template from Brandl *et al.* (2006). It is clear that the mid-IR continuum slope of the average Sy 1 spectrum is shallower than that of Sy 2, while the starburst template has the steepest spectral slope, indicating a different mixture of hot/cold dust components in these galaxies (also see Hao *et al.* 2007). This would be consistent with the interpretation that our mid-IR spectra of Sy 2s display a strong starburst contribution, possibly due to circumnuclear star-formation activity included in

the aperture from which we extracted the spectra. PAH emission, which is a good tracer of star formation activity (Förster Schreiber *et al.* 2004), can be detected in the average spectra of both Seyfert types, while it is most prominent in the average starburst spectrum. PAH emission originates from a photo-dissociation region (PDR) and can easily be destroyed by the UV/X-ray photons in a strong radiation field produced near massive stars and/or an accretion disk surrounding a SMBH.

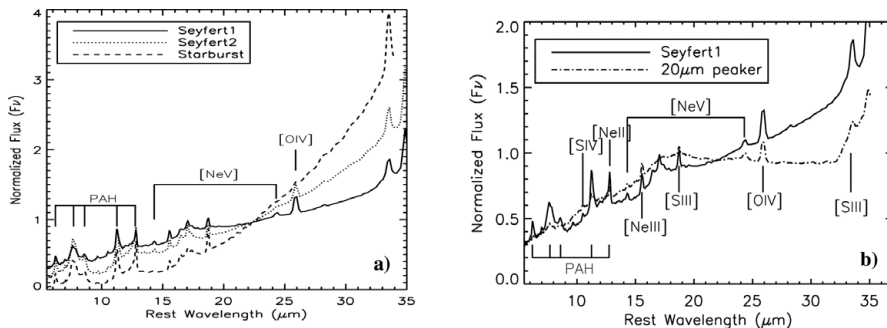


Figure 1. *Left:* A comparison among the average mid-IR spectrum of Sy 1s (solid line) and Sy 2s (dotted line) of the 12 μm sample, as well as the starbursts (dashed line) of Brandl *et al.* (2006). All spectra have been normalized at 22 μm . Note that the high-ionization fine-structure lines of [O IV] $\lambda 25.89 \mu\text{m}$ are present in all three spectra, while [Ne v] $\lambda \lambda 14.3, 24.3 \mu\text{m}$ are only present in the average spectra of the two Seyfert types. *Right:* A comparison between the average mid-IR spectrum of “20 μm peakers” (dash-dotted line) and Sy 1s (solid line) of our sample. All spectra have been normalized to the flux at 22 μm .

In the 12 μm Seyfert sample, we detect PAH emission in 37 Sy 1s and 53 Sy 2s, 78% and 93% for each type, respectively. This is expected since the apertures we used to extract the mid-IR spectra for the 12 μm sample correspond in most cases to areas of more than 1 kpc in linear dimensions. As a result, emission from the PDRs associated with the extended circumnuclear region and the disk of the host galaxy is also encompassed within the observed spectrum. High ionization fine-structure lines, such as [Ne v] $\lambda \lambda 14.32, 24.32 \mu\text{m}$, are clearly detected even in the low-resolution average Sy 1 spectrum. Since [Ne v] has an ionization potential of 97 eV, it thus serves as an unambiguous indicator of an AGN. This signature is also visible, though rather weak, in the average spectrum of Sy 2, while it is absent in the average starburst template. Even though the low-resolution mode of IRS was not designed for studying fine-structure lines, we are still able to detect [Ne v] emission in 29 Sy 1s and 32 Sy 2s, roughly 60% for both types. Another high ionization line, [O IV] $\lambda 25.89 \mu\text{m}$, with ionization potential of 54 eV, also appears in both Seyfert types (42 Sy 1s and 41 Sy 2s), and is stronger in the average spectrum of Sy 1. The [O IV] emission line can be powered by shocks in intense star-forming regions or AGNs (see Bernard-Salas *et al.* 2009; Hao *et al.* 2009, and references therein). In our sample it is probably powered by both, given the large aperture we adopted for spectral extraction. More details and a complete analysis of mid-IR fine-structure lines for 29 galaxies from the 12 μm Seyfert sample are presented by Tommasin *et al.* (2008), while the work for the entire sample is in progress (Tommasin *et al.* 2009).

A thorough examination of the spectra reveals that 15 Sy 1s and 4 Sy 2s have $F_{20}/F_{30} \geq 0.95$. We call these objects “20 μm peakers” and we display their average spectrum in Figure 1b. In addition to their characteristic continuum shape, a number of other differences between the “20 μm peakers” and Sy 1s are also evident. PAH emission, which is clearly detected in the average Sy 1 spectrum, appears to be rather weak in the average “20 μm peaker” spectrum. The high-ionization lines of [Ne v] and [O IV] are seen in both

spectra with similar strength, while low-ionization lines, especially [NeII] and [SIII], are much weaker in the average spectrum of “20 μm peakers”. If we calculate the infrared color of a galaxy using the ratio of F_{25}/F_{60} , we find an average value of 0.75 for the “20 μm peakers,” while it is 0.30 for the other “non-20 μm peaker” Sy 1s in the 12 μm sample. Finally, the average IR luminosities of the “20 μm peakers” and Sy 1s do not show significant differences, with $\log(L_{\text{IR}}/L_{\odot}) = 10.96$ for the former and $\log(L_{\text{IR}}/L_{\odot}) = 10.86$ for the latter. These results are consistent with the “20 μm peakers” being AGNs with dominant hot dust emission from a small grain population heated to effective temperatures of ~ 150 K and a possible contribution due to the distinct emissivity of astronomical silicates at 18 μm . Their radiation field must also be stronger than a typical Sy 1, since it destroys the PAH molecules around the nuclear region more efficiently (for more details, see Wu *et al.* 2009).

2.2. The PAH Emission in the 12 μm Seyferts

To quantify the strength of PAH emission, we follow the usual approach and measure the fluxes and equivalent widths (EWs) of the 6.2 and 11.2 μm PAH features from their mid-IR spectra.

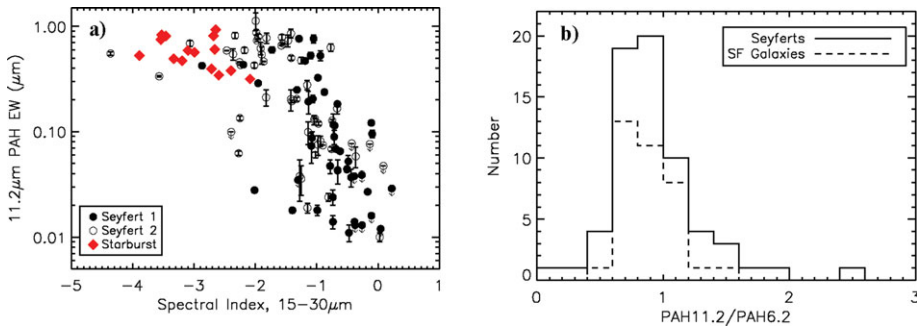


Figure 2. *Left:* The 15–30 μm spectral index vs. 11.2 μm PAH EW for the 12 μm Seyfert sample. The filled circles are Seyfert 1s, the open circles are Seyfert 2s, and the diamonds denote the starburst galaxies from Brandl *et al.* (2006). Note that the PAH EWs of Seyferts are progressively suppressed as their 15 to 30 μm continuum slopes flatten. *Right:* A histogram of the flux ratio of the 11.2 μm PAH to the 6.2 μm PAH feature. The solid line indicates the values of the 12 μm Seyfert sample, while the dashed line indicates those of the SF galaxies from Brandl *et al.* (2006) and Smith *et al.* (2007a). Galaxies with only upper limits measured for the aromatic features are excluded from this plot. Both the SF galaxies and the Seyferts appear to have similar distribution of the 11.2 $\mu\text{m}/6.2 \mu\text{m}$ PAH flux ratios, indicating that, globally, the chemical structure of the aromatic features observed in Seyfert nuclei are likely very similar to those seen in SF galaxies.

In Figure 2a, we plot the 15–30 μm spectral index for the 12 μm Seyfert sample as a function of their 11.2 μm PAH EWs. The diamonds indicate the starburst galaxies from Brandl *et al.* (2006). A general trend of the PAH EWs decreasing as a function of 15–30 μm spectral index is observed in Figure 2a, even though it is much weaker than the anti-correlation presented by Deo *et al.* (2007). Starburst galaxies are located on the upper left corner of the plot, having very steep spectral slopes, with $\langle\alpha_{15-30}\rangle = -3.02 \pm 0.50$, and large PAH EWs, nearly $0.7 \mu\text{m}$. Seyfert galaxies spread over a considerably larger range in spectral slopes as well as PAH EWs. Sy 1s and Sy 2s are mixed on the plot. On average, the 15–30 μm spectral index is $\langle\alpha_{15-30}\rangle = -0.85 \pm 0.61$ for Sy 1s and $\langle\alpha_{15-30}\rangle = -1.53 \pm 0.84$ for Sy 2s. Note that although the mean spectral slope is slightly steeper for Sy 2s, there is substantial scatter, as is evident by the uncertainties of the mean for each type.

It is well known that the flux ratio of different PAH emission bands is a strong function of PAH size and their ionization state (Draine & Li 2001). The $6.2\ \mu\text{m}$ PAH emission is due to C-C stretching mode and the $11.2\ \mu\text{m}$ feature is produced by C-H out-of-plane bending mode (Draine 2003). In Figure 2b, we display a histogram of the $11.2\ \mu\text{m}$ to $6.2\ \mu\text{m}$ PAH flux ratios for the $12\ \mu\text{m}$ Seyferts. Given the relatively small number of starburst galaxies in the Brandl *et al.* (2006) sample (16 sources), we also included 20 H II galaxies from the SINGS sample of Smith *et al.* (2007a), thus increasing the number of SF galaxies to 36 sources and making its comparison with the Seyferts more statistically meaningful. From Figure 2b, we can see that both the Seyferts and SF galaxies, indicated by the solid and dashed lines, respectively, appear to have very similar distributions of PAH $11.2\ \mu\text{m}/6.2\ \mu\text{m}$ band ratios. This implies that even though the harsh radiation field in AGNs may destroy a substantial amount of the circumnuclear PAH molecules, and does so preferentially, it likely does not do so over a large volume. Enough molecules in the circumnuclear regions do remain intact, and as a result, the aromatic features that we observe from Seyferts are essentially identical to those in SF galaxies. The relative strength of PAH emission can also be used to examine the validity of the unified AGN model that attributes the variation in AGN types to dust obscuration and relative orientation of the line of sight to the nucleus (Antonucci 1993). Sy 1s and Sy 2s are intrinsically the same but appear to be different in the optical, mainly because of the much larger extinction towards the nuclear continuum of Sy 2s when viewed edge on. The latest analysis of the IRS high-resolution spectra of 87 galaxies from the $12\ \mu\text{m}$ Seyfert sample shows that the average $11.2\ \mu\text{m}$ PAH EW is $0.29 \pm 0.38\ \mu\text{m}$ for Sy 1s and $0.37 \pm 0.35\ \mu\text{m}$ for Sy 2s (Tommasin *et al.* 2009, in preparation).

3. What Powers the $12\ \mu\text{m}$ Luminosity in the $12\ \mu\text{m}$ Seyferts?

Using the data in hand, we propose a new statistical method to estimate the AGN contribution to the total infrared luminosity of a galaxy. The method, which is presented in detail by Wu *et al.* (2009), relies on the fact that, for starforming galaxies, there is a clear correlation between the $L(11.2\ \mu\text{m PAH})$ and $L(12\ \mu\text{m continuum})$ luminosities with an average ratio $L(11.2\ \mu\text{m PAH})/L(12\ \mu\text{m continuum}) = 0.044 \pm 0.010$. Since there is no AGN contamination in the $12\ \mu\text{m}$ luminosity of star forming galaxies, we can attribute all mid-IR continuum emission to star formation. Seyfert galaxies do display a larger scatter in this ratio (see Figure 14 of Wu *et al.* 2009). However, we can decompose their $12\ \mu\text{m}$ luminosity into two parts: one contributed by the star-formation activity, which is proportional to their PAH luminosity, and one due to dust heated by the AGN. If we assume that the star-formation component in the $12\ \mu\text{m}$ luminosity of Seyferts is associated with the $11.2\ \mu\text{m}$ PAH luminosity in the same manner as in star forming galaxies, then we can estimate the star-formation contribution to the integrated $12\ \mu\text{m}$ luminosity of the Seyfert sample. Subtracting this starforming contribution from the total $12\ \mu\text{m}$ luminosity, we can obtain, in a statistical sense, the corresponding AGN contribution.

4. Conclusions

Based on the analysis of *Spitzer*-IRS low-resolution spectra for a complete unbiased sample of Seyfert galaxies selected from the *IRAS* Faint Source Catalog based on their $12\ \mu\text{m}$ fluxes, we find the following:

1. The $12\ \mu\text{m}$ Seyferts display a variety of mid-IR spectral shapes. The mid-IR continuum slopes of Sy 1s and Sy 2s are on average $\langle \alpha_{15-30} \rangle = -0.85 \pm 0.61$ and -1.53 ± 0.84 respectively, though there is substantial scatter for both types. We identify a group of

objects with a local maximum in their mid-IR continuum at $\sim 20 \mu\text{m}$, which is likely due to the presence of a warm $\sim 150 \text{ K}$ dust component and $18 \mu\text{m}$ emission from astronomical silicates. Emission lines, such as the $[\text{Ne V}] \lambda\lambda 14.3, 24.3 \mu\text{m}$ and $[\text{O IV}] \lambda 25.9 \mu\text{m}$ lines, known to be a signature of an AGN are stronger in the average spectra of Sy 1s than those of Sy 2s.

2. PAH emission is detected in both Sy 1s and Sy 2s, with no statistical difference in the relative strength of PAHs between the two types. This suggests that the volume responsible for the bulk of their emission is likely optically thin at $\sim 12 \mu\text{m}$.

3. The $11.2 \mu\text{m}$ PAH EW of the $12 \mu\text{m}$ Seyfert sample correlates well with the IRAS color of the galaxies as indicated by the flux ratio of F_{25}/F_{60} . PAH emission is more suppressed in warmer galaxies, in which the strong AGN activity may destroy the PAH molecules.

4. The FIR luminosities of the $12 \mu\text{m}$ Seyferts are dominated by star formation. Their mid-IR luminosity increases by the additional AGN contribution. A method to estimate the AGN contribution to the $12 \mu\text{m}$ luminosity, in a statistical sense, has been proposed and applied to the sample.

References

- Antonucci, R. R. J. & Miller, J. S. 1985, *ApJ*, 297, 621
 Antonucci, R. 1993, *ARAA*, 31, 473
 Bernard-Salas, J., *et al.* 2009, *ApJS*, 184, 230
 Brandl, B. R., *et al.* 2006, *ApJ*, 653, 1129
 Buchanan, C. L., *et al.* 2006, *AJ*, 132, 401
 Clavel, J., *et al.* 2000, *A&A*, 357, 839
 Deo, R. P., *et al.* 2007, *ApJ*, 671, 124
 Draine, B. T. 2003, *ARAA*, 41, 241
 Draine, B. T. & Li, A. 2001, *ApJ*, 551, 807
 Elitzur, M. 2008, *New Astron. Revs.*, 52, 274
 Förster Schreiber, N. M., Roussel, H., Sauvage, M., & Charmandaris, V. 2004, *A&A*, 419, 501
 Gorjian, V., Cleary, K., Werner, M. W., & Lawrence, C. R. 2007, *ApJ*, 655, L73
 Hao, L., *et al.* 2007, *ApJ*, 655, L77
 Hao, L., *et al.* 2009, *ApJ*, 704, 1159
 Ho, L. C. 2008, *ARAA*, 46, 475
 Houck, J. R., *et al.* 2004, *ApJS*, 154, 18
 Nenkova, M., Sirocky, M. M., Nikutta, R., Ivezić, Ž., & Elitzur, M. 2008, *ApJ*, 685, 160
 Rush, B., Malkan, M. A., & Spinoglio, L. 1993, *ApJ Sup*, 89, 1
 Smith, J. D. T., *et al.* 2007a, *ApJ*, 656, 770
 Smith, J. D. T., *et al.*, 2007b, *PASP*, 119, 1133
 Spinoglio, L. & Malkan, M. A. 1989, *ApJ*, 342, 83
 Sturm, E., *et al.* 2006, *ApJ*, 653, L13
 Thompson, G. D., Levenson, N. A., Uddin, S. A., & Sirocky, M. M. 2009, *ApJ*, 697, 182
 Tommasin, S., *et al.* 2008, *ApJ*, 676, 836
 Tommasin, S., *et al.* 2009, in preparation
 Urry, C. M. & Padovani, P. 1995, *PASP*, 107, 803
 Verma, A., Charmandaris, V., Klaas, U., Lutz, D., & Haas, M. 2005, *Space Sci. Revs.*, 119, 355
 Weedman, D. W., *et al.* 2005, *ApJ*, 633, 706
 Werner, M. W., *et al.* 2004, *ApJS*, 154, 1
 Wu, Y., Charmandaris, V., Huang, J., Spinoglio, L., & Tommasin, S. 2009, *ApJ*, 701, 658